6. E. A. Craig, M. Slater, D. Stone, H. O. Park, W. Boostein, in *RNA Polymerase and the Regulation of Transcription*, W. Reznikoff, R. Burgess, J. Dahlberg, C. Gross, T. T. Record, M. Wickens, Eds. (Elsevier, New York, 1987), p. 267.
7. M. Whiteway and J. W. Szostak, *Cell* **43**, 483 (1985).
8. T. Toda *et al.*, *Mol. Cell. Biol.* *7*, 1371 (1987).
9. P. Sass, J. Field, J. Nikawa, T. Toda, M. Wigler, *Proc. Natl. Acad. Sci. U.S.A.* **83**, 9303 (1986).
10. K. A. Borkovich and S. Lindquist, unpublished results.
11. R. A. Young and R. W. Davis, *Proc. Natl. Acad. Sci. U.S.A.* **80**, 1194 (1983).
12. S. Henikoff and M. K. Eghtedarzadeh, *Genetics* **117**, 711 (1987).
13. Y. Sanchez and S. L. Lindquist, unpublished results.
14. R. Rotstein, in *DNA Cloning, a Practical Approach*, D. M. Glover, Ed. (IRL Press, Oxford, 1985), vol. 2, p. 45.
15. DNA sequence analysis demonstrated that the clone YS121 (Fig. 2A) contained an open reading frame, beginning 210 nucleotides downstream of the Apa I site, sufficient to code for a polypeptide of 432 amino acids, with no translation termination site. When the fragment was subcloned into the centromeric yeast vector pRS316 (*16*) a heat-inducible protein of approximately 45 kD was produced. Thus, the clone contains only the NH_2-terminal half of the *HSP104* gene. To clone the missing portion of the *HSP104* gene, we use site-directed recombination and plasmid rescue (*14*). Southern (DNA) blot analysis indicated that the Eco RI–Hind III segment of *HSP104* is located between two Cla I sites that are approximately 10 kb apart in the wild-type yeast genome. Thus, the Cla I sites should encompass the entire *HSP104* gene. The Eco RI–Hind III fragment was subcloned into the integrative vector YIp5, linearized, and integrated into the chromosome by homologous recombination (Fig. 2D). Total genomic DNA from this transformant was isolated and cut with Cla I, which does not cut within the vector sequences. Digested DNA was ligated under dilute conditions and the vector, together with associated yeast chromosomal sequences, was recovered in *E. coli*. This plasmid was then used to reconstruct the entire *HSP104* gene in plasmid pYS104 (Fig. 2E).
16. R. S. Sikorski and P. Hieter, *Genetics* **122**, 19 (1989).
17. L. McAlister and D. B. Finkelstein, *Biochem. Biophys. Res. Commun.* **93**, 819 (1980).
18. G. C. Li and Z. Werb, *Proc. Natl. Acad. Sci. U.S.A.* **79**, 3281 (1982).
19. K. Watson, G. Dunlop, R. Cavicchioli, *FEBS Lett.* **172**, 299 (1984).
20. B. G. Hall, *J. Bacteriol.* **156**, 1363 (1983).
21. R. B. Widelitz, B. E. Magun, E. W. Gerner, *Mol. Cell. Biol.* **6**, 1088 (1986).
22. J. R. Subjeck, T. Shy, J. Shen, R. J. Johnson, *J. Cell. Biol.* **97**, 1389 (1983).
23. W. J. Welch and J. P. Suhan, *ibid.* **103**, 2035 (1986).
24. S. Kurtz and S. L. Lindquist, *Cell* **45**, 771 (1986).
25. G. K. Mcmaster and G. G. Carmichael, *Proc. Natl. Acad. Sci. U.S.A.* **74**, 4835 (1977).
26. L. Petko and S. L. Lindquist, *Cell* **45**, 885 (1986).
27. K. Struhl, D. T. Stinchcomb, S. Scherer, R. W. Davis, *Proc. Natl. Acad. Sci. U.S.A.* **76**, 1035 (1979).
28. B. Byers, in *The Molecular Biology of the Yeast Saccharomyces, Life Cycle and Inheritance*, J. N. Strathern, E. W. Jones, J. R. Broach, Eds. (Cold Spring Harbor Laboratory, Cold Spring Harbor, NY, 1981), p. 59.
29. We thank C. Roncero and R. Susek for discussions and helpful advice throughout this work, K. Borkovich for the antibody to hsp104, and J. Stitzel for help with sequencing. Supported by NIH grant GM 35483 and a Juan March Foundation Postdoctoral Fellowship to Y.S.

30 January 1990; accepted 2 April 1990

Cell Interactions in the Sea Urchin Embryo Studied by Fluorescence Photoablation

CHARLES A. ETTENSOHN

In many organisms, interactions between cells play a critical role in the specification of cell fates. In the sea urchin embryo, primary mesenchyme cells (PMCs) regulate the developmental program of a subpopulation of secondary mesenchyme cells (SMCs). The timing of this cell interaction was analyzed by means of a fluorescence photoablation technique, which was used to specifically ablate PMCs at various stages of development. In addition, the PMCs were microinjected into PMC-depleted recipient embryos at different developmental stages and their effect on SMC fate was examined. The critical interaction between PMCs and SMCs was brief and took place late in gastrulation. Before that time, SMCs were insensitive to the suppressive signals transmitted by the PMCs.

INTERACTIONS BETWEEN EMBRYONIC cells are an important mechanism by which cell fates are specified during development. In some organisms, including amphibians, sea urchins, and mammals, cell interactions play an especially significant role in the commitment process (*1*). Even in multicellular animals in which cell diversification is believed to be primarily under the control of cytoplasmic determinants segregated to different blastomeres during cleavage (for example, ascidians and nematodes), cell interactions are critical for the differentiation of certain cell types (*2*).

The sea urchin embryo has been a model for studying the specification of cell fate by cellular interactions. Isolated blastomeres can form complete larvae, providing evidence of regulative cell interactions that determine cell fates (*3, 4*). Cellular interactions are associated with the selection of cell fates by mesenchymal cell lineages in the sea urchin embryo. During normal ontogeny the skeletal structures of the larva are synthesized by primary mesenchyme cells (PMCs) (*5*). Late in gastrulation a second population of mesenchyme cells arises, the secondary mesenchyme cells (SMCs), which give rise to muscle cells, pigment cells, and portions of the coelomic sacs, but do not normally contribute to the larval skeleton (*3, 6*). These two cell lineages are segregated early in development, at the fourth cleavage division (7). PMC-depletion experiments indicate that an interaction takes place between the two cell populations during gastrulation (*8*). In the absence of the PMCs, 65 to 75 SMCs convert to the PMC phenotype and synthesize a complete larval skeleton. Therefore, SMCs can form skeletal structures, but this pathway of differentiation is normally suppressed by the PMCs. The suppression of SMC skeletogenesis is quantitatively dependent on the number of PMCs in the blastocoel. If at least 50 PMCs are present, SMC conversion is completely blocked. If fewer than 50 PMCs are present, the number of SMCs that express a skeletogenic phenotype is inversely proportional to the number of PMCs in the blastocoel (*9*). I now show that the critical interaction between the PMCs and SMCs is brief and occurs late in gastrulation, at the time the SMCs enter the blastocoel and begin to migrate.

The timing of the interaction between PMCs and SMCs was determined by means of a fluorescence photoablation technique that was used to specifically eliminate the PMCs at different stages of development. In previous experiments, microsurgical methods were used to remove PMCs from embryos immediately after their formation (*9*). At later stages of embryo development, this approach is impractical because the PMCs disperse within the blastocoel and adhere firmly to the basal surfaces of overlying epithelial cells. Therefore to ablate PMCs at later stages, endogenous populations of PMCs were removed microsurgically and replaced with equal numbers of PMCs that had been covalently labeled with rhodamine B isothiocyanate (RITC) (*10*). The fluorescently tagged PMCs were then selectively ablated at different developmental stages by irradiating the embryos with green light (λ_{max} = 550 nm). Previous studies have shown that rhodamine-labeled PMCs microinjected into the blastocoel of recipient embryos undergo normal migration and spiculogenesis (*11*). Such transplanted PMCs completely suppress the conversion of SMCs to a skeletogenic phenotype when microinjected into PMC-depleted embryos, provided that at least 50 cells are transplanted (*9*).

Other studies have used fluorescence methods to ablate embryonic cells by mi-

Department of Biological Sciences, Carnegie Mellon University, Pittsburgh, PA 15213.

croinjecting fluorescent dextrans into early blastomeres followed by the photoablation of the labeled progeny at later developmental stages (*12*). Direct labeling of embryonic cell surfaces by covalent coupling reagents (isothiocyanates, succinimidyl esters, and other reagents) provides an alternative to intracellular microinjection of fluorescent labels and may be useful in labeling large populations of cells (such as for cell recombination experiments carried out in tissue culture), cells that are difficult to microinject, or cells whose precursors have not been identified.

The efficacy of the photoablation technique in eliminating rhodamine-labeled PMCs was demonstrated in four ways. (i) Direct observation of rhodamine-labeled PMCs during exposure to 550-nm light revealed that irradiation was accompanied by rapid changes in cell shape (retraction of cell processes) and a change in the general appearance of the cytoplasm of the labeled cells from transparent to opaque and granular (Fig. 1). (ii) After irradiation at 550 nm, RITC-labeled cells stained with trypan blue, an indication that they were no longer viable. (iii) Examination of fixed embryos revealed that photoablation caused labeled PMCs to aggregate in large masses and blocked spicule formation by the RITC-labeled cells (Fig. 2). (iv) Photoablation at early stages resulted in a complete conversion response, demonstrating that the donor PMCs had been functionally eliminated (Figs. 2 and 3).

Immunoreactivity with the monoclonal antibody (MAb) 6a9 was used as a marker for SMC conversion. This antibody recognizes the sulfated glycoprotein msp130, a cell surface protein normally expressed only by PMCs (*9, 13*). SMCs do not exhibit detectable levels of 6a9 immunoreactivity in normal embryos (*9*). Converted SMCs were counted after whole mounts of embryos were stained with MAb 6a9 and a fluorescein-conjugated secondary antibody (Fig. 2). Donor (rhodamine-labeled) PMCs exhibited both red and green fluorescence, while converted SMCs exhibited only green fluorescence.

Exposure of unlabeled embryos to light at 550 nm for 4 min neither induced (in the case of control embryos) nor blocked (in the case of PMC-deficient embryos) the conversion response, which was monitored by staining with MAb 6a9. Embryos that contained a mixture of rhodamine-labeled and unlabeled PMCs were used to determine the selectivity of the photoablation procedure. In such embryos, rhodamine-labeled donor PMCs that were adjacent to unlabeled host PMCs could be selectively destroyed by exposure to 550-nm light (as monitored by cell shape changes and trypan blue staining) without affecting adjacent cells. These observations indicated that the photoablation procedure was effective in ablating the PMCs without otherwise affecting development.

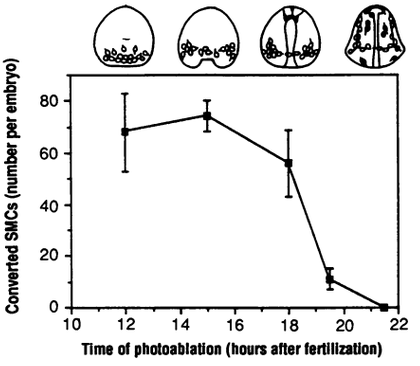

Fig. 3. Fluorescence photoablation. Numbers of converted SMCs were determined by immunofluorescent staining with MAb 6a9. Embryos were photoablated at various developmental stages and fixed 22 hours after PMC ingression, after the completion of SMC conversion. PMC ingression in *L. variegatus* takes place 10 hours after fertilization at 24°C. The developmental stages of the embryos at the time of photoablation are illustrated. Bars indicate standard errors (95% confidence limits on the mean). For each developmental stage, 5 to 11 embryos were scored.

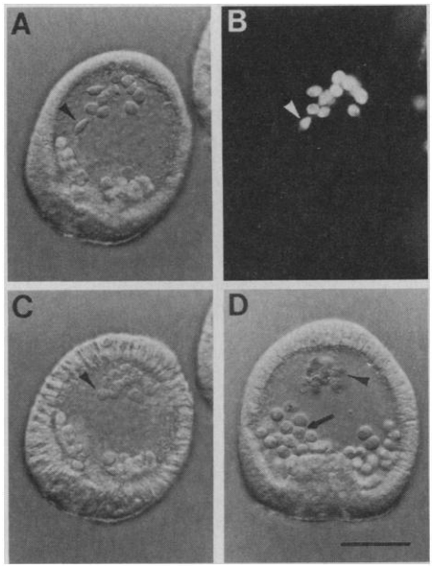

Fig. 1. Fluorescence photoablation of RITC-labeled PMCs. These micrographs show a living *L. variegatus* mesenchyme blastula microinjected with 11 rhodamine-labeled PMCs. The PMCs of the recipient embryo have been left in the blastocoel in order to demonstrate the selectivity of the photoablation for labeled PMCs. (**A** and **B**) The recipient embryo at the start of a 2-min irradiation, photographed with differential interference contrast (A) and epifluorescence (B) optics. The arrowhead indicates a PMC with a bipolar shape and filopodial processes. (**C**) The same embryo immediately after the photoablation. The cytoplasm of the labeled PMCs has become granular, and the bipolar PMC (arrowhead) has retracted its processes. Photoablation also results in a transient change in the contours of the embryo. (**D**) One hour after the photoablation, the contours of the embryo have smoothed. The photoablated PMCs are opaque and clumped in a single mass (arrowhead). The unlabeled PMCs of the recipient embryo are migrating normally (arrow). Bar represents 50 μm.

Photoablation of the PMCs even 8 hours after ingression resulted in a nearly complete conversion response (>50 SMCs expressing the msp130 epitope recognized by MAb 6a9) (Fig. 3). By this late stage of gastrulation the PMCs had completed their migratory phase, arranged themselves in a well-formed ring pattern with two ventrolateral clusters, and initiated the synthesis of the embryonic skeleton. Even by this stage no irreversible interaction had taken place between the PMCs and SMCs. Photoablation of the PMCs 8 to 10 hours after ingression

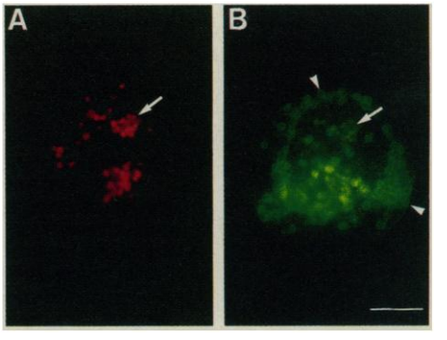

Fig. 2. SMC conversion after fluorescence photoablation of PMCs. This embryo was depleted of PMCs at the mesenchyme blastula stage and microinjected with 50 to 60 RITC-labeled PMCs. The embryo was then released from the microinjection chamber and allowed to develop for 4 hours more. It was then placed in a microinjection chamber, and the labeled PMCs were photoablated by irradiating the embryo at 550 nm for 4 min. The embryo was released from the chamber and allowed to develop for an additional 5 hours, then fixed in ice-cold 100% methanol (20 min), rinsed four times in ice-cold ASW, and stained for indirect immunofluorescence with MAb 6a9 and fluorescein-conjugated goat antiserum to mouse immunoglobulin G antibody (1:50 in ASW) (Organon Teknica). The embryo was squashed between two cover slips and photographed with epifluorescence optics. (**A**) Rhodamine fluorescence. The photoablated PMCs are fragmented and scattered in clumps in the blastocoel (arrow), and spicule formation by these cells is blocked. In control embryos, PMCs are aligned along extensive, branched skeletal rods. (**B**) Fluorescein fluorescence. Photoablation of the PMCs has resulted in the conversion of SMCs to the skeletogenic phenotype. The converted PMCs (arrowheads) express the msp130 glycoprotein and have arranged themselves in a ring pattern like that formed by PMCs. Arrow indicates corresponding positions of photoablated PMCs shown in (A). Bar represents 50 μm.

resulted in intermediate numbers of converted cells. If PMCs were photoablated at the prism stage (10 to 12 hours after ingression), SMCs no longer converted. The period of sensitivity in these experiments corresponded to the stage of SMC ingression and migration (Fig. 3), and suggests that the critical signal passes between the PMCs and SMCs at this time.

The above results are consistent with three hypotheses. (i) The PMCs transmit a signal continuously throughout gastrulation (for example, PMCs may produce a suppressor molecule that is secreted continuously). (ii) The PMCs do not send an inhibitory signal until late in gastrulation, perhaps because they have not completed their own program of differentiation until that time. (iii) The SMCs are not competent to respond to the relevant signal until the late gastrula stage. This could be the case regardless of the temporal pattern of PMC signaling.

To distinguish among these alternatives, PMCs were removed from mesenchyme blastulae and the PMC-depleted embryos were allowed to develop for progressively longer periods of time before 50 to 60 rhodamine-labeled PMCs were reintroduced into the blastocoel by microinjection (Fig. 4A). Twenty-four hours after fertilization, the embryos were fixed as whole mounts and stained by indirect immunofluorescence with MAb 6a9. These experiments show that the continuous presence of the PMCs is not required for suppression of the skeletogenic potential of the SMCs (Fig. 4B). Injection of PMCs into the blastocoel at the late mesenchyme blastula or early gastrula stage (11 and 13.5 hours after fertilization, respectively) resulted in complete inhibition of SMC conversion (Fig. 4B). Reintroduction of PMCs as late as the mid-gastrula stage, 6 to 7 hours after PMC depletion and only 3 hours before the initiation of conversion as assayed by MAb 6a9 immunoreactivity, led to a reduction in the numbers of converted cells ($\bar{x}$ = 25.7, n = 11) although SMC conversion was not completely blocked.

The above data rule out the hypothesis that PMCs must transmit a signal continuously during gastrulation. SMC conversion was largely suppressed in less than 3 hours, and complete suppression occurred in 3 to 6 hours. In addition, since the donor PMCs used in the transplantation experiments were taken from developmentally young mesenchyme blastula-stage embryos, these results do not support the hypothesis that the PMCs are not developmentally competent to transmit a signal until the late gastrula stage, unless the experimental conditions induced the PMCs to undergo an accelerated morphogenetic program and transmit the correct signal early. Although PMCs reintroduced into the blastocoel 3 hours before SMC ingression largely suppressed conversion, the photoablation data showed that PMCs can be present in the blastocoel for much longer periods during earlier stages of gastrulation without suppressing SMC skeletogenesis (Fig. 3).

The above observations indicate that the critical interaction between PMCs and SMCs is brief and takes place late in gastrulation, at the time when SMCs leave the tip of the archenteron and migrate into the blastocoel. Inhibitory cues are apparently established by the PMCs earlier, but the prospective SMCs are not sensitive to them. In addition, the PMC signal is transient and decays rapidly upon ablation of the PMCs. These observations may indicate that the SMCs become developmentally committed when they ingress into the blastocoel and convert to a skeletogenic phenotype unless they interact with viable PMCs at that time.

Whatever the specific mechanism of this inhibitory interaction, the result is the suppression of a complex battery of phenotypic responses on the part of the converting SMCs. The earliest indication of conversion that we have detected is the de novo expression of cell surface molecules normally characteristic of the PMCs (*9*). Later, converted SMCs migrate to sites along the blastocoel wall normally occupied by the PMCs and secrete a complete larval skeleton. Skeletal spicules are complex structures composed of $CaCO_3$, $MgCO_3$, and several acidic glycoproteins deposited intracellularly within a syncytial network of cell processes (*14*). It is likely that cell lineage conversion involves changes in cell surface properties, ion transport, protein trafficking, and biosynthetic patterns on the part of the SMCs. The PMCs need not migrate normally, occupy their typical sites on the blastocoel wall, or synthesize spicules in order to suppress SMC skeletogenesis (*15*). We are currently testing the possibility that extracellular matrix molecules secreted by the PMCs (*16*) participate in mediating this cell-cell interaction and whether direct filopodial contact between these two populations of migratory cells is required for signaling.

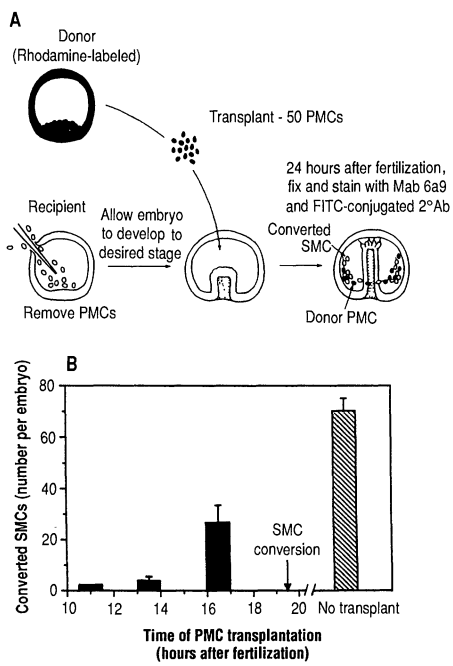

Fig. 4. SMC commitment. (**A**) PMCs were removed from recipient embryos at the mesenchyme blastula stage (10 hours after fertilization). The embryos were allowed to continue development for various times, then were loaded again into microinjection chambers and 50 to 60 RITC-labeled PMCs from mesenchyme blastula stage donor embryos were microinjected into the blastocoel. At 24 hours after fertilization (14 hours after PMC ingression) embryos were fixed and stained by indirect immunofluorescence with MAb 6a9. (**B**) The time (in hours after fertilization) at which labeled PMCs were introduced into the blastocoel and the numbers of converted SMCs. The number of SMCs that convert in embryos in which no PMCs are present is approximately 70. The start of SMC conversion as determined by immunofluorescent staining of PMC-depleted embryos with MAb 6a9 is shown. Error bars indicate 95% confidence limits on the mean. For each developmental stage, 5 to 11 embryos were scored.

REFERENCES AND NOTES

1. E. H. Davidson, *Gene Activity in Early Development*, (Academic Press, New York, 1986).
2. J. Kimble, *Dev. Biol.* **87**, 286 (1981); P. W. Sternberg and H. R. Horvitz, *Cell* **44**, 761 (1984); P. W. Sternberg, *Nature* **335**, 551 (1988); H. Nishida and N. Satoh, *Dev. Biol.* **132**, 355 (1989).
3. S. Hörstadius, *Experimental Embryology of Echinoderms* (Clarendon Press, Oxford, 1973).
4. M. Spiegel and E. Spiegel, *Am. Zool.* **15**, 583 (1975); F. H. Wilt, *Development* **100**, 559 (1987); E. H. Davidson, *ibid.* **105**, 421 (1989).
5. K. Okazaki, in *The Sea Urchin Embryo: Biochemistry and Morphogenesis*, G. Czihak, Ed. (Springer-Verlag, New York, 1975), pp. 177–232; M. A. Harkey, in *Time, Space, and Pattern in Embryonic Development*, R. Raff and W. Jeffrey, Eds. (Liss, New York, 1983), pp. 131–155; M. Solursh, in *Developmental Biology*, L. Browder, Ed. (Plenum, New York, 1986), pp. 391–431; D. R. McClay and C. A. Ettensohn, *Symp. Soc. Develop. Biol.* **45**, 111 (1987); G. L. Decker and W. J. Lennarz, *Development* **103**, 231 (1988).
6. T. Gustafson and L. Wolpert, *Biol. Rev.* **42**, 442 (1967); C. A. Ettensohn, unpublished observations.
7. R. A. Cameron, B. R. Hough-Evans, R. J. Britten, E. H. Davidson, *Genes Dev.* **1**, 75 (1987).
8. S. Hörstadius, *Acta Zool.* **9**, 1 (1928); T. Fukushi, *Bull. Marine Biol. Stat. Asamushi* **11**, 21 (1962); R. E. Langelan and A. H. Whiteley, *Dev. Biol.* **109**, 464 (1985); C. A. Ettensohn and D. R. McClay, *ibid.* **125**, 396 (1988).
9. C. A. Ettensohn and D. R. McClay, *Dev. Biol.* **125**, 396 (1988).
10. *Lytechinus variegatus* embryos were raised to the mesenchyme blastula stage (10 hours after fertilization, 24°C) in artificial seawater (ASW). Donor embryos were fluorescently labeled with freshly made RITC (rhodamine B isothiocyanate, mixed isomers, Sigma No. R1755). RITC (2 mg) was dissolved in 20 μl of dimethyl sulfoxide, and ASW

(5 ml) was added gradually to this solution while vortexing. The solution was vortexed an additional 2 min and then passed through a 0.45-μm pore size syringe filter (Gelman Scientific); 50 to 150 μl was added to 10 ml of ASW in a 60-mm petri dish and several drops of a concentrated embryo suspension were added. The dish was placed in the dark for 1 hour, then the embryos were washed several times over 30 min with ASW and placed in microinjection chambers (*11*). In separate chambers, PMCs of unlabeled recipient embryos were removed by directing a gentle flow of ASW into the blastocoel through a micropipette (*9*). RITC-labeled PMCs were removed from donor embryos and 50 to 60 cells were microinjected into each PMC-depleted recipient with a beveled siliconized microneedle attached to a pressure injection apparatus (*11*). Previous studies have shown that 50 PMCs are a sufficient number to completely suppress SMC skeletogenesis (*9*). After the microsurgery (a 1/2- to 1-hour procedure), embryos were placed in depression slides in humid dishes and development continued. At intervals, the embryos were collected with a mouth pipette, placed again in microinjection chambers, and then irradiated (2 to 4 min) (100-watt mercury arc lamp of Nikon Diaphot epifluorescence microscope; Nikon G-1B cube, with 546/10 nm excitation filter, 580 nm dichroic mirror, and 590 nm barrier filter). In each trial, 15 to 30 PMC-depleted embryos were allowed to develop in parallel with embryos that had received PMC transplants. Some of these PMC-depleted embryos were fixed and processed for indirect immunofluorescence at the time of photoablations. These embryos served as an internal control to confirm that conversion as monitored by MAb 6a9 immunoreactivity had not begun at the time of photoablation.

11. C. A. Ettensohn and D. R. McClay, *Dev. Biol.* **117**, 380 (1986).
12. M. Shankland, *Nature* **307**, 541 (1984); H. Nishida and N. Satoh, *Dev. Biol.* **132**, 355 (1989).
13. D. D. Carson *et al.*, *Cell* **41**, 639 (1985); J. A. Anstrom *et al.*, *Development* **101**, 255 (1987); D. S. Leaf *et al.*, *Dev. Biol.* **121**, 29 (1987); M. C. Farach-Carson *et al.*, *J. Cell Biol.* **109**, 1289 (1989).
14. S. C. Benson, N. Crise-Benson, F. Wilt, *J. Cell Biol.* **102**, 1878 (1986); G. L. Decker and W. J. Lennarz, *Development* **103**, 231 (1988).
15. C. A. Ettensohn, unpublished observations. PMC migration and spiculogenesis can be blocked by microinjecting wheat germ agglutinin into living embryos. SMC conversion is completely suppressed in such embryos.
16. J. Blankenship and S. Benson, *Exp. Cell Res.* **152**, 98 (1984); L. M. Angerer *et al.*, *Genes Dev.* **2**, 239 (1988), S. Benson, L. Smith, F. Witt, R. Shaw, *Exp. Cell Res.* **188**, 141 (1990).

17. I thank A. Koretsky, D. McClay, and W. McClure for valuable discussions. Supported by a NSF presidential young investigator award, a Basil O'Connor Starter Scholar Award from the March of Dimes Foundation, and NIH grant HD24690.

26 December 1989; accepted 12 March 1990

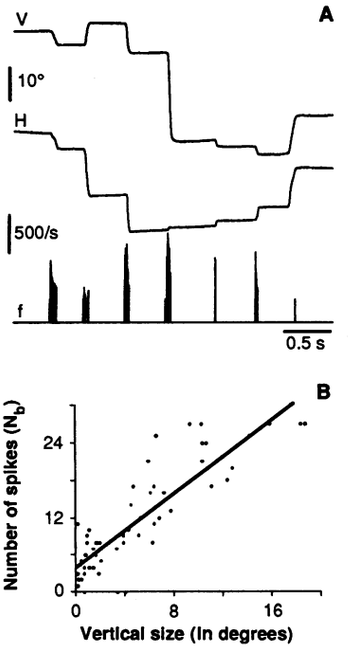

Fig. 1. (**A**) Discharge pattern of one typical VMLB; f, firing rate; H, instantaneous horizontal eye position; V, instantaneous vertical eye position. (**B**) The number of spikes in the burst of one VMLB (n_b) as a function of amplitude of downward components of saccades or vertical size (v). A straight line described by the equation $n_b = 1.49v + 4.04$ was fitted through points that represent downward saccades ($r = 0.86$).

A Structural Basis for Hering's Law: Projections to Extraocular Motoneurons

ADONIS K. MOSCHOVAKIS, CHARLES A. SCUDDER,* STEVEN M. HIGHSTEIN

Conjugate eye movements are executed through the concurrent activation of several muscles in both eyes. The neural mechanisms that underlie such synergistic muscle activations have been a matter of considerable experimentation and debate. In order to investigate this issue, the projections of a class of primate premotoneuronal cells were studied, namely, the vertical medium-lead burst neurons (VMLBs), which drive vertical rapid eye movements. Axons of upward VMLBs ramify bilaterally within motoneuron pools that supply the superior rectus and inferior oblique muscles of both eyes. Axons of downward VMLBs ramify ipsilaterally in the inferior rectus portion of the oculomotor nucleus and in the trochlear nucleus. Thus, VMLBs can drive vertical motoneuron pools of both eyes during conjugate vertical rapid eye movements; these data support Hering's law.

ORDINARY MOTOR ACTIVITY depends on the coactivation of synergistic muscle groups. A special case of this phenomenon is encountered in the oculomotor system where extraocular muscles of both eyes must be coactivated if the resulting eye movements are to be conjugate (that is, for both eyes to move simultaneously in the same direction and by the same amount). Over a century ago, Hering proposed a mechanism to account for eye conjugacy known as Hering's Law of Equal Innervation (*1*). According to this law, the two eyes move in a conjugate manner because they receive identical signals from the brain (equal innervation). Hering suggested that there was equal outflow in the nerves innervating the separate extraocular muscles. Because it is now known that each motoneuron pool innervates only one muscle (*2*), the issue is whether, and how, the motoneuron pools that innervate the separate muscles receive equal innervation. The known synaptic organization of the oculomotor system has not thus far offered a satisfying validation of Hering's principle. A stronger validation would be obtained if branches from a single neuron to separate motoneuron pools could be demonstrated.

A. K. Moschovakis, Laboratory of Neural Control, National Institute of Neurological Diseases and Stroke, Bethesda, MD 20892.
C. A. Scudder and S. M. Highstein, Department of Otolaryngology, Washington University School of Medicine, St. Louis, MO 63110.

*To whom correspondence should be addressed.

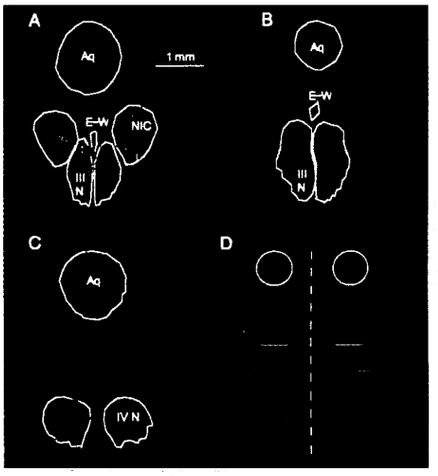

Fig. 2. (**A** through **C**) Frontal plots of the terminal fields distributed in the rostral (A) and caudal (B) half of the oculomotor nucleus and in the trochlear (C) nucleus by one upward (blue) and one downward (red) VMLB that were intraaxonally injected with HRP in alert, behaving primates. (**D**) Bilateral schematic diagram of the organization of the vertical saccadic system (eyes indicated by open circles, the midline by dashes). Arrows indicate the projections of up (blue) and down (red) VMLBs, as well as up (blue) and down (red) motoneurons. III N, oculomotor nucleus; IV N, trochlear nucleus; Aq, aqueduct; E-W, Edinger-Westphal nucleus; NIC, interstitial nucleus of Cajal; IO, inferior oblique; IR, inferior rectus; SO, superior oblique; SR, superior rectus.